Direct Growth of Short Single-Walled Carbon Nanotubes with Narrow-Chirality Distribution by Time-Programmed Plasma Chemical Vapor Deposition

Toshiaki Kato* and Rikizo Hatakeyama

Department of Electronic Engineering, Tohoku University, Aoba 6-6-05, Aramaki-Aza, Aoba-Ku, Sendai 980-8579 (Japan)

ABSTRACT We have realized the direct growth of the short-length (<100 nm) single-walled carbon nanotubes (SWNTs) with a narrow-chirality distribution by time-programmed plasma chemical vapor deposition (TP-PCVD). Transmission electron microscope and atomic force microscope analyses reveal that the very short (<100 nm) SWNTs are selectively grown by precisely controlling their growth time on the order of a few seconds. Direct photoluminescence excitation measurements also show that the chirality distribution of the short SWNTs is fairly narrow, and (7, 6) and (8, 4) dominant short SWNTs are successfully synthesized by TP-PCVD.

KEYWORDS: single-walled carbon nanotubes · short length · chirality · plasma CVD

Single-walled carbon nanotubes (SWNTs)[1] have attracted much attention as one of the most promising nanomaterials with exceptional electronic and structural properties. Since the electronic and optical properties of SWNTs strongly depend on the tube diameter (d_t) and the chirality, it is important to selectively grow SWNTs with a narrow d_t and (n, m) chirality distribution. A lot of effort has been dedicated to this issue, and some progress has been made by several groups.[2−6]

The length of SWNTs is another very important factor which determines the SWNT properties. Recently, the length-controlled SWNTs, especially the short-length SWNTs, have attracted intense attention because of their unique features, such as ballistic electron transport,[7] blue shift of optical band gap due to quantum confinement along the axial direction,[8] high-frequency mechanical resonator,[9] molecular sensing,[10] biological imaging,[11] and drug delivery.[11] However, compared to the study on the radial structure control, such as the d_t and chirality, very few efforts have been devoted toward the axial structure control, *i.e.*, the length control of SWNTs, especially to the short SWNTs. Furthermore, a simultaneous control of both the radial (d_t and chirality) and axial (length) structures still remains to be a major challenge in the fundamental studies and applications of SWNTs.

There are two main approaches to obtain the short-length SWNTs. One is a direct growth, and the other is a method based on the post treatments, such as cuttings[12] and chemical separations.[13] Almost all of the works reported thus far use the later one, which is based on the top down process. Ultrashort (<10 nm) SWNTs[8] are fabricated by the combination of chemical cutting and separation. However, the obtained SWNTs by these top down approaches are contaminated by abrasive materials employed in some processes, and the use of chemicals and surfactants inhibits the intrinsic property characterization of SWNTs due to their reaction and interaction. On the other hand, the directly grown short SWNTs can maintain their original high quality and clean surface without any chemical impurities, which makes it possible to fully utilize their potential abilities in various application fields. Very recently, the direct growth of the short SWNTs[14] has been reported. However, the control of diameter and chirality of the directly grown short SWNTs has not been realized yet, which is necessary for the fabrication of high-performance electrical and optical devices with the short-length SWNTs.

Here, we report a novel direct growth approach of the short-length SWNTs based on time-programmed plasma chemical vapor deposition (TP-PCVD). By precisely

*Address correspondence to kato12@ecei.tohoku.ac.jp.

Received for review September 13, 2010 and accepted November 11, 2010.

Published online November 17, 2010. 10.1021/nn102379p

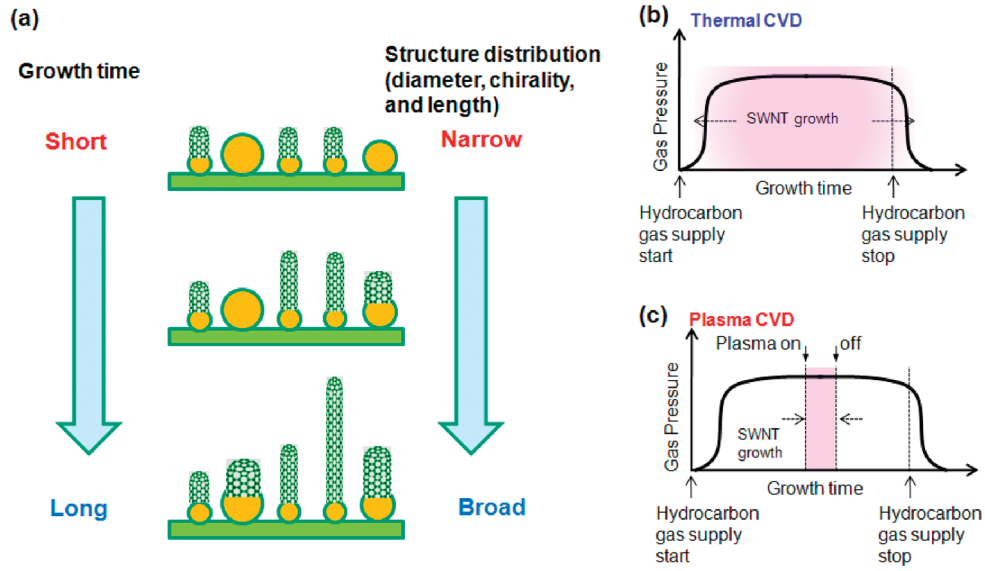

Figure 1. Schematic illustration of time-programmed plasma CVD. (a) Structure distribution of SWNTs at different growth times. Typical time schemes of SWNT growth with (b) thermal and (c) plasma CVD.

adjusting the growth time (t_g), the length distribution is narrowed, and the short-length (<100 nm) SWNTs are successfully grown for a very short growth time (2−5 s). Furthermore, the direct photoluminescence (PL) study reveals that the short-length SWNTs have the (7, 6) and (8, 4) dominant narrow-chirality distribution. This is the first report for the direct growth of the short-length SWNTs with a narrow-chirality distribution. Biomolecules, such as DNA, are known to react with a specific chirality SWNT.[15] Freestanding short-length SWNTs are very stable under the various environments, such as air condition and solution phase. Therefore our produced freestanding as-grown short SWNTs with narrow-chirality distribution are expected to contribute to the fabrication of high-performance biomolecule sensors.

RESULTS AND DISCUSSION

Figure 1a shows a basic concept of our approach. Recent progress in the *in situ* transmission electron microscope (TEM) observation during SWNT growth revealed that metal-catalyzed SWNT growth is initiated by the formation of a carbon cap structure on the surface of a catalytic nanoparticle with a certain incubation time (t_i).[16] Although the detailed mechanism in this incubation period is still argued, it is expected that there might be correlations between the t_i and SWNT structures, such as d_t and chirality. When we assume that the t_i of the small d_t (or specific chirality) SWNTs is shorter than that of the larger (or other chiralities) one, it should be possible to selectively grow the narrow-d_t (or chirality) distributed SWNTs by strictly controlling the t_g at their initial growth stage (Figure 1a). Since the length of SWNTs should be proportional to the growth time at the initial growth stage, the very short SWNTs can be obtained by adjusting the growth time. Chemical vapor deposition (CVD), thermal and plasma CVD, is one of the most promising SWNT production methods, which has advantages, such as a large scale production and a direct site-assigned growth. In the case of thermal CVD, the SWNT growth gradually starts and stops after the initiation of feeding and pumping the hydrocarbon gas, respectively (Figure 1b). The growth time in thermal CVD includes some uncertainness, which makes it difficult to be used for a precise growth time control. In the case of plasma CVD, on the other hand, reactive ions and radicals are main species for the nanotubes growth, and the SWNT growth is carried out only when a plasma is generated. This suggests that the growth time can be controlled by timing an electric power supply used for the plasma generation (Figure 1c), and the precise t_g control on the order of microsecond is possible in plasma CVD. Based on this strategy, we attempt to grow the narrow-d_t and -chirality distributed short SWNTs by precisely adjusting the t_g with TP-PCVD. Although plasma CVD is a well-known SWNT growth method, which has benefits in low-temperature[17] and freestanding growth,[18] there is not any report focusing on this high controllability of the growth time.

The length distribution of SWNTs is carefully investigated by TEM and atomic force microscopy (AFM). In the case of the relatively long time (~ 60 s) growth, the length distribution of SWNTs is broad (Figure 2a and c). On the contrary, when the growth time is carefully controlled on the order of a few seconds, almost all the SWNTs are very short (<100 nm), and the distribution is also narrowed, which is confirmed by the direct TEM observation (Figure 2b) and the AFM characterization (Figure 2d) (see Experimental Methods Section). This indicates that it is possible to directly grow the short SWNTs by precisely adjusting the growth time by TP-

PCVD. Interestingly, when we compare the radial breathing mode (RBM) in Raman scattering spectra, a clear difference is also observed. In the case of the long-time growth, many kinds of the RBM peaks appear (Figure 2e), whereas only one specific peak is observed in the short-time growth sample (Figure 2f).

In order to analyze the chirality distribution of the short SWNTs in detail, we carry out the PL excitation (PLE) map analysis. It is to be noted that since our plasma CVD grown SWNTs take on the freestanding form due to the strong electric field in the plasma sheath area during their growth, it is possible to observe PL signals from as-grown SWNTs on a substrate.[19] All the PLE measurements are carried out immediately after the growth to prevent SWNTs from forming thin bundles, which leads to causing the PL intensity change by exciton energy transfer between each tube.[19] From the density estimation of SWNTs with the direct TEM observations, it is confirmed that abundant SWNTs exist in the area where the PLE measurement is carried out. Thus, the PLE map gives us macroscopic information in each sample. Figure 3a−c shows the PLE maps of the as-grown SWNTs as a function of t_g. SWNT populations for each d_t are also plotted by calculating with the PL intensity and quantum efficiency[20] (Figure 3d−f). It is found that the d_t distribution just after the incubation (2 s) is relatively narrow, and the main diameter is about 0.8 nm with (6, 5), (7, 5), (7, 6), (8, 4), and (9, 2) dominant chiralities (Figure 3a, d, and g). Then, the relatively large d_t (0.95 nm) SWNTs [(8, 6) and (9, 4)] initiate their growth at 5 s (Figure 3b, e, and 3h). The larger d_t SWNTs of (8, 7) are finally grown at 10 s, where the chirality and the d_t distributions are broad (Figure 3c, f, and i). The small end of the d_t does not change, whereas the large end increases with an increase in the t_g. Significant dependence of chiral angle and type (type 1: $(2n + m)$ mod 3 = 1, type 2: $(2n + m)$ mod 3 = 2)[21] on the t_g is not found in this experiment (Figure 3g, h, and i). In more detail, when we plot the t_i as a function of the d_t, a clear dependence is obtained (Figure 3j). It is to be noted that the t_i of each chirality is defined as the t_g when a clear PL signal is first observed (Figure 3a−c). The t_i increases with an increase in the tube diameter, which supports the validity of our basic concept described in Figure 1a.

To further narrow the initial d_t and chirality distributions, we adjust the other growth conditions. Figure 4 shows the PLE map dependence on the growth temperature of SWNTs grown for the very short growth time (2 s). Interestingly, when we decrease the growth temperature down to 600 °C the chirality distribution is very narrowed, and (7,6) and (8,4) SWNTs are predominantly grown (Figure 4c). At the lower growth temperature (≤580 °C), SWNTs could not be grown for the very short growth time (2 s). However, similar narrow-chirality distributed SWNTs are grown by extending the growth time until 15 s (see Supporting Information). This indicates that the t_i for each d_t and chirality is sensitive to the growth temperature. It should be also emphasized that the chirality distribution just after the t_i is always narrowly independent of other growth parameters. The narrow-chirality distributed SWNTs growth by TP-PCVD is reproducibly obtained (see Supporting Information). This is the first result of the direct growth of the short-length SWNTs with a narrow-chirality distribution.

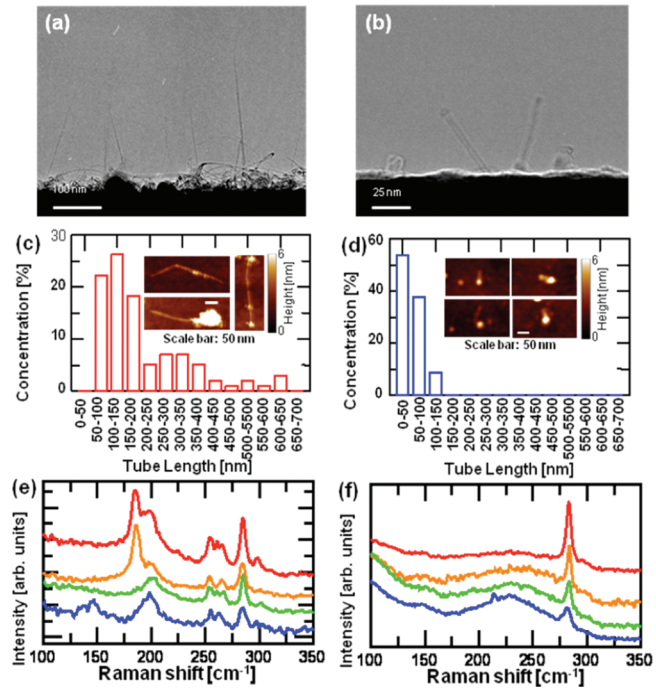

Figure 2. Length distribution of SWNTs. (a and b) TEM images of freestanding SWNTs produced by long (a) and short (b) growth times. (c and d) Length distributions of SWNTs measured by AFM for (c) long and (d) short time growths. Inset shows typical AFM images of SWNTs. The total number of SWNTs measured for the histograms of (c) and (d) are 99 and 69, respectively. (e and f) Typical RBM in Raman scattering spectra of SWNTs produced for (e) long and (f) short growth times. Each spectrum is taken at a different position on the same substrate.

The most important factor for the narrow-chirality distributed growth of short SWNTs by TP-PCVD is to control the d_t dependence on t_i for each chirality SWNT. If each t_i largely varies depending on the d_t or chirality of SWNT, then it is possible to more selectively grow the specific chirality SWNTs by adjusting the growth time. As shown in Figure 4, the growth temperature is one of the key factors to cause the t_i variation for each d_t SWNT. The cap formation process might be one of the critical reasons for this temperature dependence. The central part of the graphene sheet formed on the top of catalyst surface has to lift off the catalytic particle for the growth of SWNTs. This can only happen if the kinetic energy per area at the interface between the graphene sheet and the catalyst (E_{kin}) is high enough to overcome the work of adhesion per area of graphite toward the catalytic particle (W_{ad}) ($E_{kin} > W_{ad}$).[22] Small tubes have lower W_{ad}.[23] Since the E_{kin} should be proportional to the growth temperature, the producible type

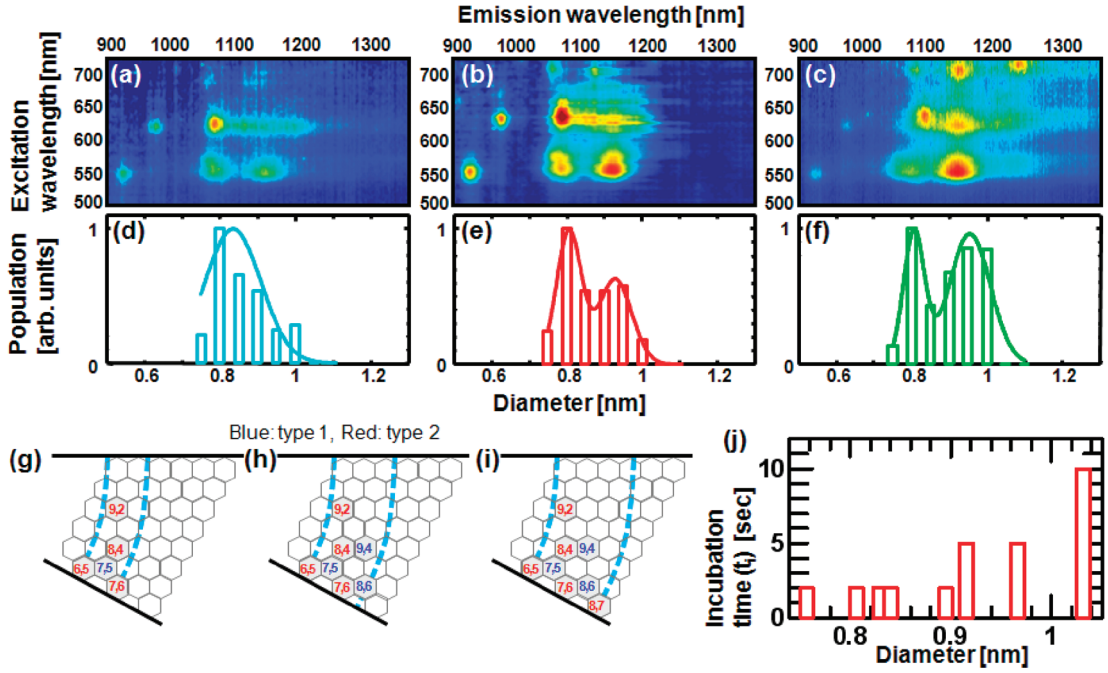

Figure 3. Chirality and diameter distributions of SWNTs as a function of growth time. (a−c) PLE maps of SWNTs produced by the different growth time, which is (a) 2 s, (b) 5 s, and (c) 10 s. (d−f) Population of SWNTs as a function of the tube diameter, which is calculated by the PL intensity and quantum efficiency [(d) 2 s, (e) 5 s, and (f) 10 s]. (g−i) Chirality maps in a graphene segment as a function of the growth time [(g) 2 s, (h) 5 s, and (i) 10 s]. Dotted lines show the minimum and maximum diameter range for each sample. (j) Plot of the incubation time as a function of the tube diameter.

of SWNTs under the low-growth temperature condition can be highly selected compared with that in the higher growth temperature.

As we have discussed above, the growth temperature is one of the key parameters to realize the narrow-chirality distribution of SWNTs by TP-PCVD. In order to realize the further precise control of the d_t and chirality distribution, it is an inevitable issue to reveal the critical factor, which causes the d_t dependence on the t_i. The catalyst particle-size variation during the heating process might be one possibility. If the catalyst aggregation is enhanced during the growth process, then the chirality distribution also changes. To investigate this issue, we carry out the PLE mapping measurement of SWNTs grown for the different preheating time (see Supporting Information). After heating the substrate up to 620 °C, the temperature is kept for certain times (0, 30, and 60 s), and then similar TP-PCVD is carried out. If the catalyst particle size distribution varies during the heating process and this is the critical factor of the d_t dependence on t_i, then clear differences should appear in the PLE map of SWNTs grown under the different preheating conditions. In any preheating time, however, the d_t and chirality distribution does not show obvious changes. This indicates that the catalyst size distribution is almost the same during the short time growth (Figures 3a−c), and its effect is negligible for the d_t dependence on t_i (Figure 3j).

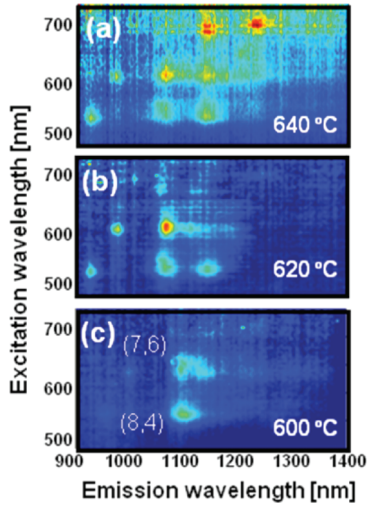

Figure 4. Growth temperature dependence of the PLE-maps of SWNTs grown for very short growth time (2 s). The growth temperature of (a−c) is 640, 620, and 600 °C, respectively.

The other possibility to cause the d_t dependence on the t_i is a supersaturation time difference. Since the SWNTs growth is carried out following a supersaturation of carbons in a catalyst, it is expected that the small catalysts are rapidly supersaturated with carbon atoms prior to the case of the large catalysts. To confirm this effect, we carry out the PLE map measurement of SWNTs grown under the low-hydrocarbon supply condition. If the supersaturation time difference is the critical factor to cause the d_t dependence on the t_i, then the selectivity of d_t or chirality should be improved by decreasing the hydrocarbon supply. The amount of the hydrocarbon supply is controlled by adjusting the radio frequency (RF, 13.56 MHz) power (P_{RF}) used for the plasma generation. The t_i clearly increases up to 20 s by

decreasing the amount of hydrocarbon supply (P_{RF} = 25 W), which should be caused by the longer supersaturation period of carbons in the catalyst at their initial growth stage. However, various kinds of chirality species of SWNTs equally start their growth, and the selective growth of narrow-d_t or -chirality distributed SWNTs is not observed under this low-hydrocarbon supply condition (see Supporting Information). Although the t_i for whole SWNTs is sensitive to the hydrocarbon supply, the selectivity of d_t or chirality is found to be conducted by the other factors. A simple estimation based on the carbon atom numbers also supports the validity of this explanation. The soluble carbon atoms in a typical 1 nm Fe catalyst (Fe_{50}) are about 26−27.[24] On the other hand, the number of carbon atoms constructing a 1 nm d_t and 100 nm length SWNT is about 2.35×10^4. Judging from this carbon atom number, it is difficult to selectively achieve the supersaturation only for the d_t = 0.8 nm with 100 nm length SWNT prior to the d_t = 0.95 nm SWNT (Figure 3j).

As we have just demonstrated, the low-temperature growth is one of the necessary conditions for the narrow-chirality distributed short SWNTs growth by TP-PCVD. However, it is not the sufficient condition, and the other factor is required. To reveal the other critical factor, which influences the d_t or chirality distribution in TP-PCVD, we precisely investigate the plasma parameters between these two conditions, where the chirality distribution of SWNTs at the initial growth stage is narrow (P_{RF} = 200 W) and broad (P_{RF} = 25 W). As we have just discussed, although the amount of the hydrocarbon supply is one of the clear differences under these two conditions, it is not critical for the d_t dependence on t_i. Through the detailed plasma analysis, it is found that there is a clear difference between these two plasma conditions, which is a plasma sheath electric field ($\boldsymbol{E}_{sh}$). We estimate the $\boldsymbol{E}_{sh}$ on the surface of substrate by solving the Poisson's equation (see Supporting Information).[25] For the simplification, we apply a dc sheath model.[25] We use the values of several plasma parameters, such as electron density, electron temperature, space potential, and floating (= substrate potential) potential, as the initial conditions to solve the equation, which are given by Langmuir prove measurements. The calculation is carried out by the Mathematica program. In the case of the high-hydrocarbon supply condition, where the narrow-chirality distribution is realized, the $\boldsymbol{E}_{sh}$ is $\sim 1.7 \times 10^4$ V/m. On the other hand, the $\boldsymbol{E}_{sh}$ is $\sim 6.7 \times 10^2$ V/m in the case of the low-hydrocarbon supply condition, where the chirality and diameter distribution is broad. This is about 25 times weaker than that of the high-hydrocarbon supply condition. In general, it is believed that the cap structure of SWNTs determines the chirality of nanotubes. Under the same diameter condition, the number of the stable cap structure is limited due to the isolated pentagon rule.[26] It is also reported that the electron energy state of the cap structure of SWNT is highly modified under the strong electric field.[27] Based on these reasons, it is conjectured that the strong electric field in the plasma sheath might have certain effects on the growth of SWNTs, especially in the cap nucleation period, which can promote the selective growth of specific chirality SWNTs resulting in the d_t dependence on t_i. Although further theoretical and computational studies are required to completely reveal the electric field effects on the nucleation of SWNTs, we believe that the unique plasma sheath effect includes a possibility to realize the growth of specific chirality SWNTs with high selectivity.

CONCLUSIONS

We have realized the direct growth of the short-length SWNTs with the narrow-chirality distribution by TP-PCVD. The length distribution of SWNTs grown for a short time is fairly narrow, and almost all the SWNTs are very short (<100 nm). In addition, the precise time-restricted growth reveals that there is a clear dependence of the d_t on t_i. Furthermore, the chirality distribution is narrowed by strictly controlling their growth time at the initial stage, and (7, 6) and (8, 4) dominant narrow-chirality distributed short-length SWNTs are directly synthesized by TP-PCVD.

EXPERIMENTAL METHODS

Single-Walled Carbon Nanotube Growth. A homemade plasma CVD unit was utilized for the growth of single-walled carbon nanotubes (SWNTs). Fe film deposited on an Al_2O_3/Ag substrate was utilized as a catalyst for the SWNT growth. The growth time was precisely controlled by a radio frequency (RF, 13.56 MHz) power supply system. The substrate was set on a heater, and a chamber was evacuated by reaching below 10^{-1} Pa with a rotary and diffusion pump. Then the substrate was heated up to a desired temperature under the 50 Pa hydrogen condition. A mixture of methane and hydrogen with 3/7 flow rate was supplied after reaching the suitable growth temperature, and the condition was kept for 1 min to make the system stabilized. RF power (P_{RF}) was then supplied for the desired growth time. After turning off the RF power supply, methane and hydrogen mixture gases were immediately evacuated, and Ar was fed during a cooling process. The samples were taken out after the temperature went down below 70 °C. Typical growth conditions are as follows: P_{RF} = 200 W, electrode−substrate distance = 700 mm, substrate temperature = 580−640 °C, and growth time = 2∼15 s.

Photoluminescence Excitation Spectroscopy. The as-grown samples on the substrates were directly utilized to take a photoluminescence excitation (PLE) map. PLE measurements were performed by a Nanolog (Horiba/Jobin yvon). A 450 W xenon lamp was used to supply the excitation light in the 500−800 nm range in 4 nm steps. The photoluminescence (PL) spectra were recorded using a liquid nitrogen-cooled InGaAs array detector in the 900−1400 nm range under the room temperature condition. The slit width used for the emission and excitation was 10 nm. It should be noted that all the PLE measurements are carried out immediately after the growth to prevent SWNTs from forming thin bundles, which leads to causing the PL intensity change by exciton energy transfer between each tube.

Length Estimation with Atomic Force Microscopy. SWNTs were dispersed in *N*-methylpyrrolidone with an ultrasonic homogenizer. Then, a piece of Si substrate was soaked in the solution and rinsed with water and dried. The Si substrate was pretreated with 3-aminopropyltriethoxysilane (APTES, 12 mL in 20 mL H_2O) to enhance the adsorption of SWNTs. Tapping mode atomic force microscopy (AFM, JEOL JSPM-5400) was used to acquire images of SWNTs on the substrate under ambient conditions.

Direct Transmission Electron Microscopy Observation. In order to estimate the SWNT length, we carried out the direct observation of as-grown state of SWNTs by transmission electron microscopy (TEM, Hitachi HF-2000). SWNTs were grown on a thin Cu wire (diameter = 100 μm) covered by the multilayer catalyst (Fe/Al_2O_3). Then, the thin Cu wire was carefully transferred to the TEM holder without any post treatments, and the surface of the thin Cu wire was observed.

Raman Scattering Spectroscopy. Raman scattering spectra were taken by a micro-Raman scattering spectroscopy (Horiba) with 632.8 nm He−Ne laser excitation.

Acknowledgment. This work was supported by JSPS-CAS Core-University Program on Plasma and Nuclear Fusion. We are grateful to Prof. K. Tohji and Mr. K. Motomiya for their help with TEM observation.

Supporting Information Available: Systematical PLE investigations. Potential profile calculation in the plasma sheath. This material is available free of charge *via* the Internet at http://pubs.acs.org.

REFERENCES AND NOTES

1. Iijima, S.; Ichihashi, T. Single-Shell Carbon Nanotubes of 1-nm Diameter. *Nature* **1993**, *363*, 603–605.
2. Bachilo, S. M.; Balzano, L.; Herrera, J. E.; Pompeo, F.; Resasco, D. E.; Weisman, R. B. Narrow (n,m)-Distribution of Single-Walled Carbon Nanotubes Grown Using a Solid Supported Catalyst. *J. Am. Chem. Soc.* **2003**, *125*, 11186–11187.
3. Miyauchi, Y.; Chiashi, S.; Murakami, Y.; Hayashida, Y.; Maruyama, S. Fluorescence Spectroscopy of Single-Walled Carbon Nanotubes Synthesized from Alcohol. *Chem. Phys. Lett.* **2004**, *387*, 198–203.
4. Li, X.; Tu, X.; Zaric, S.; Welsher, K.; Seo, W. S.; Zhao, W.; Dai, H. Selective Synthesis Combined with Chemical Separation of Single-Walled Carbon Nanotubes for Chirality Selection. *J. Am. Chem. Soc.* **2007**, *129*, 15770–15771.
5. Chiang, W.-H.; Sankaran, R. M. Linking Catalyst Composition to Chirality Distributions of As-Grown Single-Walled Carbon Nanotubes by Tuning Ni_xFe_{1-x} Nanoparticles. *Nat. Mater.* **2009**, *8*, 882–886.
6. Ghorannevis, Z.; Kato, T.; Kaneko, T.; Hatakeyama, R. Narrow-Chirality Distributed Single-Walled Carbon Nanotube Growth from Nonmagnetic Catalyst. *J. Am. Chem. Soc.* **2010**, *132*, 9570–9572.
7. Javey, A.; Guo, J.; Wang, Q.; Lundstrom, M.; Dai, H. Ballistic Carbon Nanotube Field-Effect Transistors. *Nature* **2003**, *424*, 654–657.
8. Sun, X.; Zaric, S.; Daranciang, D.; Welsher, K.; Lu, Y.; Li, X.; Dai, H. Optical Properties of Ultrashort Semiconducting Single-Walled Carbon Nanotube Capsules Down to Sub-10 nm. *J. Am. Chem. Soc.* **2008**, *130*, 6551–6555.
9. Garcia-Sanchez, D.; San Paulo, A.; Esplandiu, M. J.; Perez-Murano, F.; Forro, L.; Aguasca, A.; Bachtold, A. Mechanical Detection of Carbon Nanotube Resonator Vibrations. *Phys. Rev. Lett.* **2007**, *99*, 085501.
10. Ziegler, K. J.; Gu, Z. N.; Shaver, J.; Chen, Z. Y.; Flor, E. L.; Schmidt, D. J.; Chan, C.; Hauge, R. H.; Smalley, R. E. Cutting Single-Walled Carbon Nanotubes. *Nanotechnology* **2005**, *16*, S539–S544.
11. Liu, Z.; Tabakman, S.; Welsher, K.; Dai, H. Carbon Nanotubes in Biology and Medicine: In Vitro and In Vivo Detection, Imaging and Drug Delivery. *Nano Res.* **2009**, *2*, 85–120.
12. Chen, Z. Y.; Kobashi, K.; Rauwald, U.; Booker, R.; Fan, H.; Hwang, W. F.; Tour, J. M. Soluble Ultra-Short Single-Walled Carbon Nanotubes. *J. Am. Chem. Soc.* **2006**, *128*, 10568–10571.
13. Fagan, J. A.; Becker, M. L.; Chun, J.; Hobbie, E. K. Length Fractionation of Carbon Nanotubes Using Centrifugation. *Adv. Mater.* **2008**, *20*, 1609–1613.
14. Liu, B.; Ren, W.; Liu, C.; Sun, C.-H.; Gao, L.; Li, S.; Jiang, C.; Cheng, H.-M. Growth Velocity and Direct Length-Sorted Growth of Short Single-Walled Carbon Nanotubes by a Metal-Catalyst-Free Chemical Vapor Deposition Process. *ACS Nano* **2009**, *3*, 3421–3430.
15. Tu, X.; Manohar, S.; Jagota, A.; Zheng, M. DNA Sequence Motifs for Structure-Specific Recognition and Separation of Carbon Nanotubes. *Nature* **2009**, *460*, 250–253.
16. Hofmann, S.; Sharma, R.; Ducati, C.; Du, G.; Mattevi, C.; Cepek, C.; Cantoro, M.; Pisana, S.; Parvez, A.; Cervantes-Sodi, F.; et al. *In situ* Observations of Catalyst Dynamics during Surface-Bound Carbon Nanotube Nucleation. *Nano Lett.* **2007**, *7*, 602–608.
17. Kato, T.; Jeong, G.-H.; Hirata, T.; Hatakeyama, R.; Tohji, K.; Motomiya, K. Single-Walled Carbon Nanotubes Produced by Plasma-Enhanced Chemical Vapor Deposition. *Chem. Phys. Lett.* **2003**, *381*, 422–426.
18. Kato, T.; Hatakeyama, R.; Tohji, K. Diffusion Plasma Chemical Vapor Deposition Yielding Freestanding Individual Single-Walled Carbon Nanotubes on a Silicon-Based Flat Substrate. *Nanotechnology* **2006**, *17*, 2223–2226.
19. Kato, T.; Hatakeyama, R. Exciton Energy Transfer-Assisted Photoluminescence Brightening from Freestanding Single-Walled Carbon Nanotube Bundles. *J. Am. Chem. Soc.* **2008**, *130*, 8101–8107.
20. Oyama, Y.; Saito, R.; Sato, K.; Jiang, J.; Samsonidze, G. G.; Gruneis, A.; Miyauchi, Y.; Maruyama, S.; Jorio, A.; Dresselhaus, G.; et al. Photoluminescence Intensity of Single-Wall Carbon Nanotubes. *Carbon* **2006**, *44*, 873–879.
21. Bachilo, S. M.; Strano, M. S.; Kittrel, C.; Hauge, R. H.; Smalley, R. E.; Weisman, R. B. Structure-Assigned Optical Spectra of Single-Walled Carbon Nanotubes. *Science* **2002**, *298*, 2361–2366.
22. Ding, F.; Bolton, K.; Rosen, A. Nucleation and Growth of Single-Walled Carbon Nanotubes: A Molecular Dynamics Study. *J. Phys. Chem. B* **2004**, *108*, 17369–17377.
23. Kanzow, H.; Lenski, C.; Ding, A. Single-Wall Carbon Nanotube Diameter Distributions Calculated from Experimental Parameters. *Phys. Rev. B: Condens. Matter Mater. Phys.* **2001**, *63*, 125402−1–6.
24. Ding, F.; Larsson, P.; Larsson, J. A.; Ahuja, R.; Duan, H.; Rosen, A.; Bolton, K. The Importance of Strong Carbon-Metal Adhesion for Catalytic Nucleation of Single-Walled Carbon Nanotubes. *Nano Lett.* **2008**, *8*, 463–468.
25. Lieberman, M. A.; Lichtenberg, A. J. *Principles of Plasma Discharges and Materials Processing*; Wiley: New York, 1994; pp 154−190.
26. Kroto, H. W. The Stability of the Fullerenes Cn, with n = 24, 28, 32, 36, 50, 60 and 70. *Nature* **1987**, *329*, 529–531.
27. Kim, C.; Kim, B.; Lee, S. M.; Jo, C.; Lee, Y. H. Effect of Electric Field on the Electronic Structures of Carbon Nanotubes. *Appl. Phys. Lett.* **2001**, *79*, 1187–1189.